

# PNAS

www.pnas.org

Supplementary Information for

**Screen Identifies DYRK1B Network as Mediator of Transcription Repression on Damaged Chromatin**

Chao Dong, Kirk L. West, Xin Yi Tan, Junshi Li, Toyotaka Ishibashi, Cheng-han Yu, Shirley M.H. Sy, Justin W.C. Leung<sup>#</sup>, Michael S.Y. Huen<sup>#</sup>

<sup>#</sup>correspondence:

Michael S.Y. Huen [huen.michael@hku.hk](mailto:huen.michael@hku.hk)

Justin W.C. Leung [jwleung@uams.edu](mailto:jwleung@uams.edu)

**This PDF file includes:**

Figures S1 to S11  
Tables S1 to S5

Figure S1

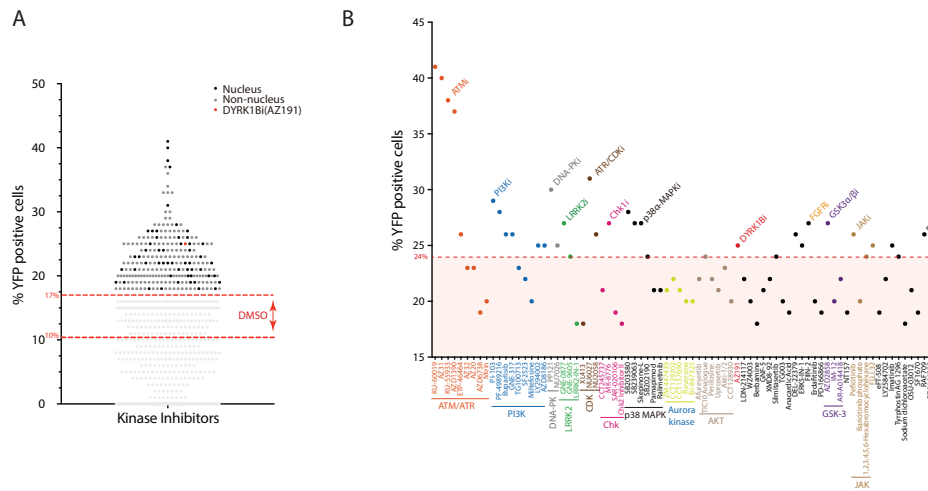


**Figure S1 Kinase inhibitor library screen reveals novel activities in DSB-induced transcription suppression**

**A)** Graphical display of kinase inhibitor targets and their corresponding percentage of cells with YFP-MS2 focus. Experimental variation in percentage of cells with YFP-MS2 focus following induction of DSBs was 10 - 17%; **B)** Chemical inhibitors that target nuclear kinases were selected and grouped based on cell percentage of YFP-MS2 focus (>17%). We applied a stringent cutoff at 24% for better presentation of candidate kinases in DISC.

Figure S2

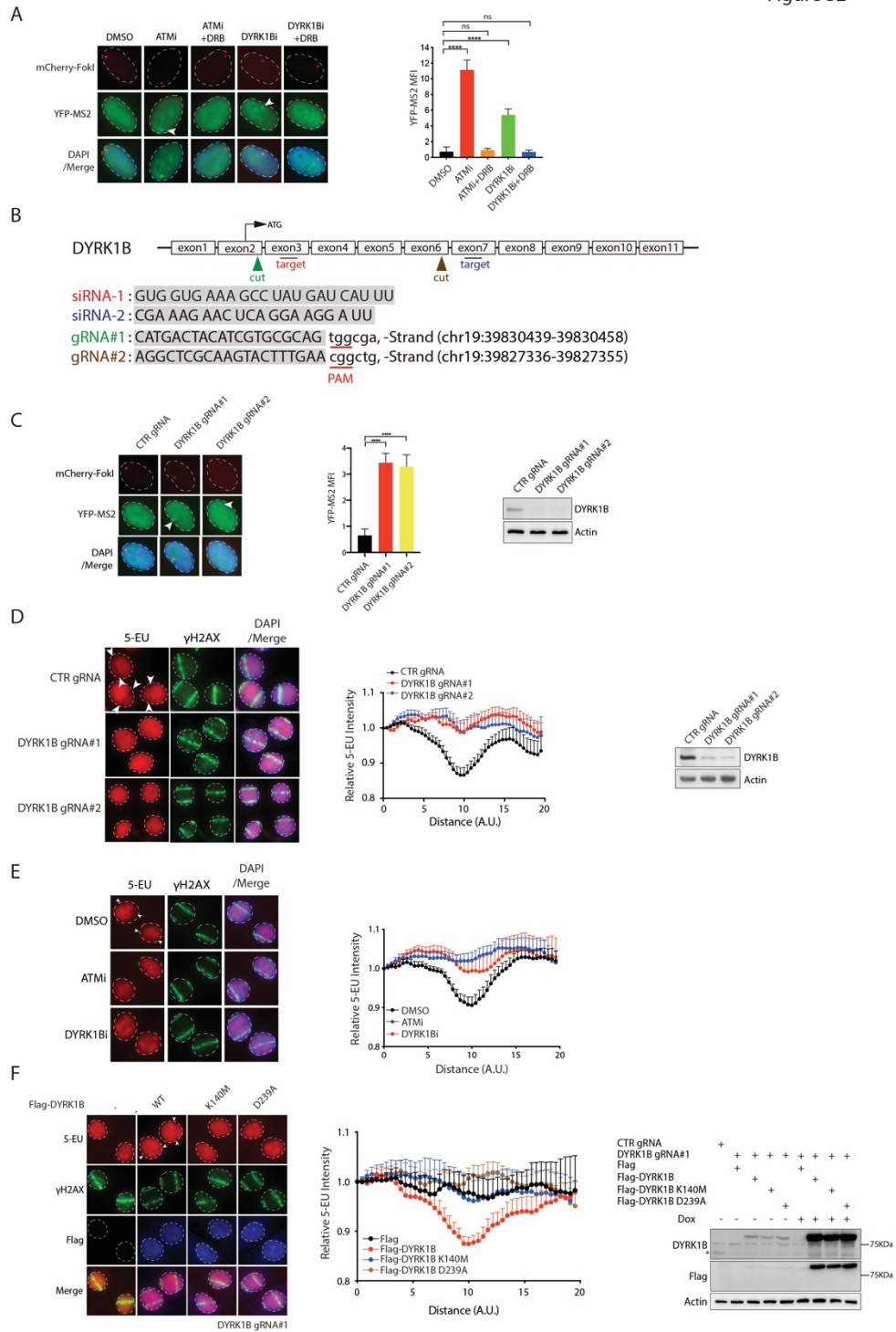


**Figure S2 DYRK1B promotes transcription silencing on DSB-flanking chromatin**

**A)** Defective DISC in DYRK1B inhibited cells is suppressed by DRB. U2OS-DSB reporter cells pre-treated with DMSO or chemical inhibitors that target ATM (ATMi; KU55933) or DYRK1B (DYRK1Bi; AZ191) were incubated with or without the transcription elongation inhibitor DRB prior to processing for visualisation and quantification of YFP-MS2 focus. Bars represent mean  $\pm$  SEM; \*\*\*\* $P < 0.0001$ ; ns, not significant; **B)** Schematic illustration of DYRK1B gene locus, sequences of DYRK1B-targeting siRNAs and gRNAs and their corresponding target. Note that exons are not presented in actual size proportion; **C)** U2OS-DSB reporter cells were lenti-virally transduced with control (CTR gRNA) or DYRK1B-targeting gRNAs (DYRK1B gRNA#1 and DYRK1B gRNA#2). Transduced cells were induced with Dox, 4-OHT and Shield-1 and were processed and quantified as in **(A)**. Western blotting was performed to assess DYRK1B silencing efficiency; **D)** HeLa cells were lenti-virally transduced with control (CTR gRNA) or DYRK1B-targeting gRNAs (DYRK1B gRNA#1 and DYRK1B gRNA#2). Transduced cells were processed for laser microirradiation and immunostaining to assess 5-EU incorporation.  $\gamma$ H2AX labels laser-induced DSBs and nuclei were counterstained with DAPI. Relative 5-EU intensity is plotted and is derived from at least 20 cells from two independent experiments. Bars represent mean  $\pm$  SEM. Western blotting was performed to assess DYRK1B silencing efficiency using indicated antibodies; **E)** HeLa cells pre-treated with ATM inhibitor (ATMi; KU55933) or DYRK1B inhibitor (DYRK1Bi; AZ191) were processed for laser microirradiation and immunostaining to assess 5-EU incorporation as in **(D)**. Bars represent mean  $\pm$  SEM; **F)** DYRK1B-silenced cells reconstituted with Dox-inducible expression vector (TRE-Vector-Flag) or those that harbour DYRK1B alleles were induced with doxycycline. 24 hr post treatment cells were microirradiated and processed for laser microirradiation and immunostaining to assess 5-EU incorporation as in **(D)**. Bars represent mean  $\pm$  SEM. Western blotting was performed to examine expression of DYRK1B using indicated antibodies. Asterisk denotes protein band that corresponds to endogenous DYRK1B.

Figure S3

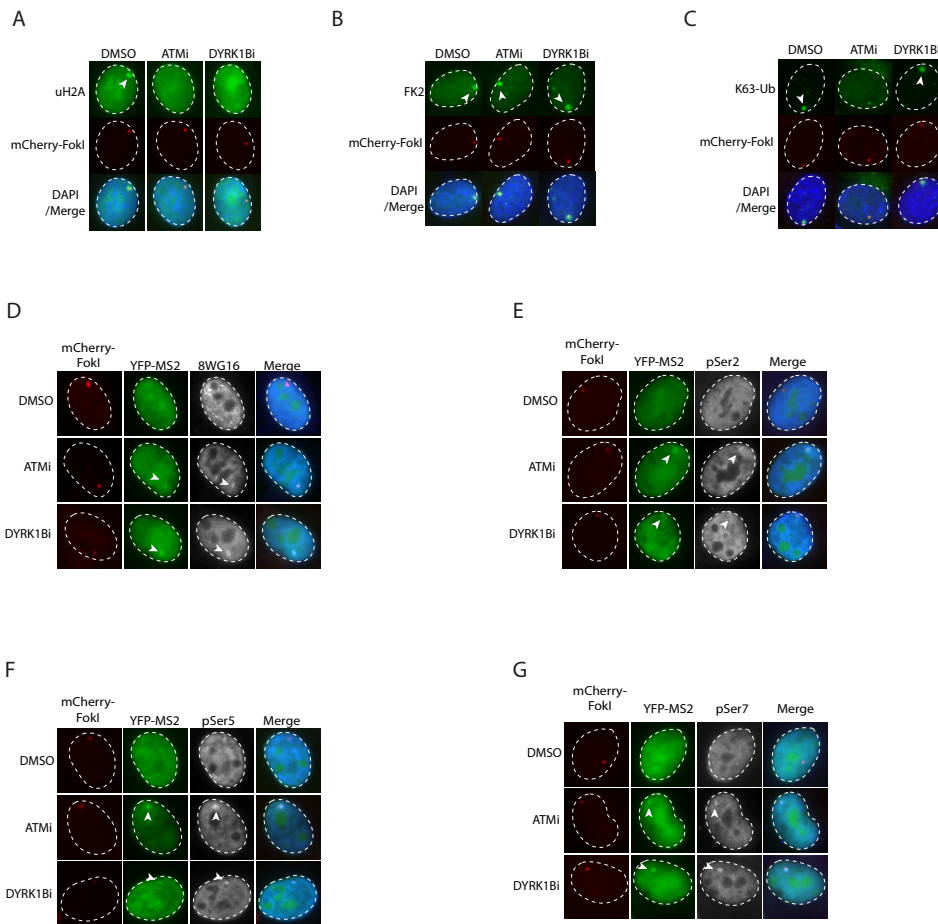


**Figure S3 DYRK1B promotes ATM-dependent DISC**

**A - G**) Chemical inhibition of DYRK1B attenuates ATM-dependent chromatin change at DSBs. U2OS-DSB reporter cells pre-treated with DMSO, ATM inhibitor (ATMi; KU55933) or DYRK1B inhibitor (DYRK1Bi; AZ191) were induced with Dox, 4-OHT and Shield-1. Cells were fixed and processed for immunostaining experimentations using indicated antibodies.

Figure S4

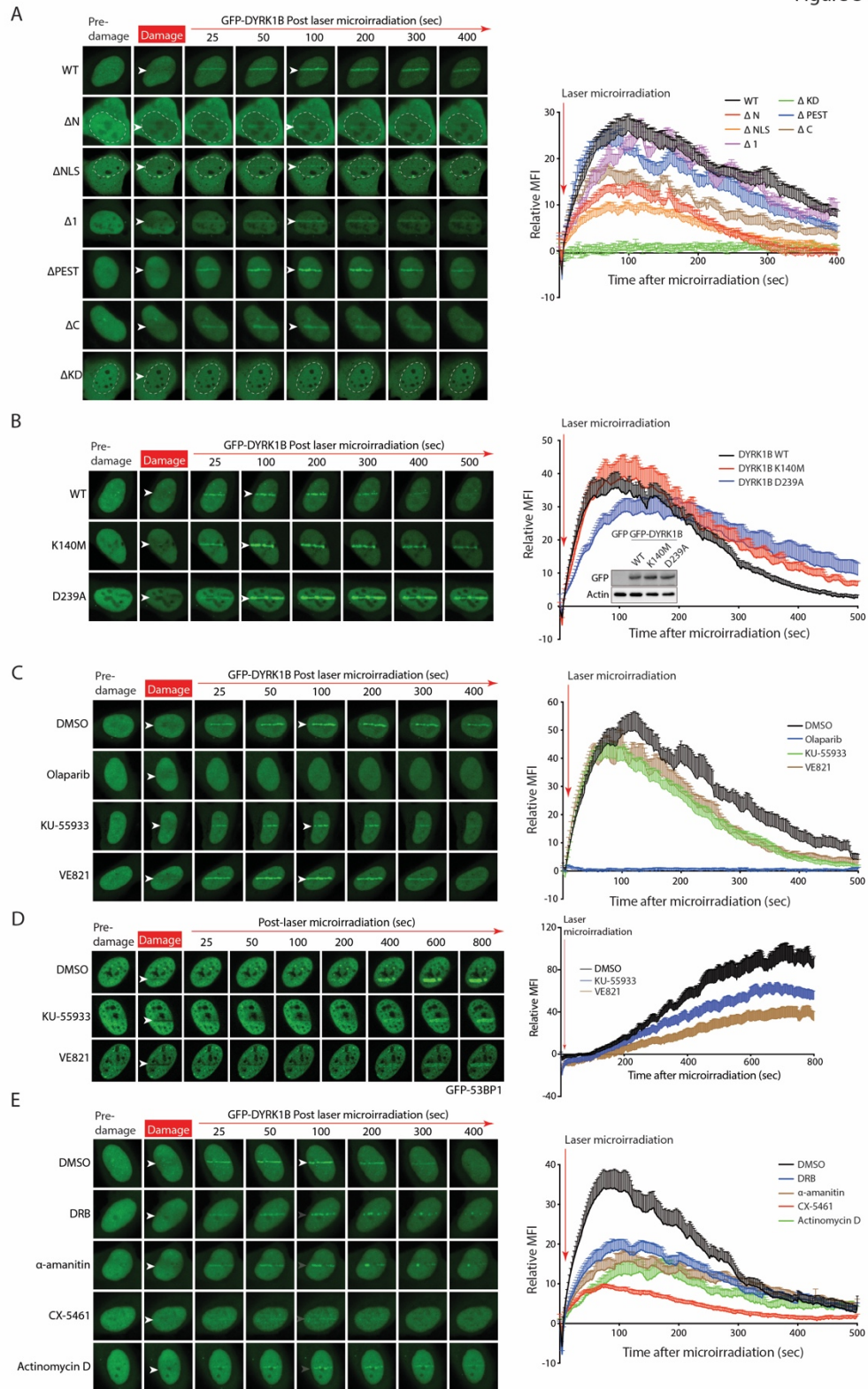


**Figure S4 Accumulation of GFP-DYRK1B at laser-induced DNA damage tracks**

**A)** Cells expressing GFP-DYRK1B alleles were laser microirradiated and time-lapse images were captured to analyse protein accumulation at DNA damage tracks. Quantification of DSB accumulation of GFP-DYRK1B wildtype (WT) and mutants is presented. Arrowheads denote sites of laser-induced DNA damage. Refer to **Figure 3B** for DYRK1B alleles; **B)** Cells expressing GFP-DYRK1B wildtype (WT) or its phospho-mutants (K140M and D239A) were processed as in **(A)**; **C & E)** Cells expressing GFP-DYRK1B were pre-treated with indicated inhibitors prior to laser microirradiation and processing for time-lapse imaging to determine DYRK1B accumulation at DSBs. Quantification of GFP-DYRK1B is shown and is derived from analyses of at least 10 cells from two independent experiments. Bars represent mean  $\pm$  SEM; **D)** Cells expressing GFP-53BP1 were pre-treated with DMSO or indicated inhibitors prior to laser microirradiation and were processed as in **(A)**.

Figure S5

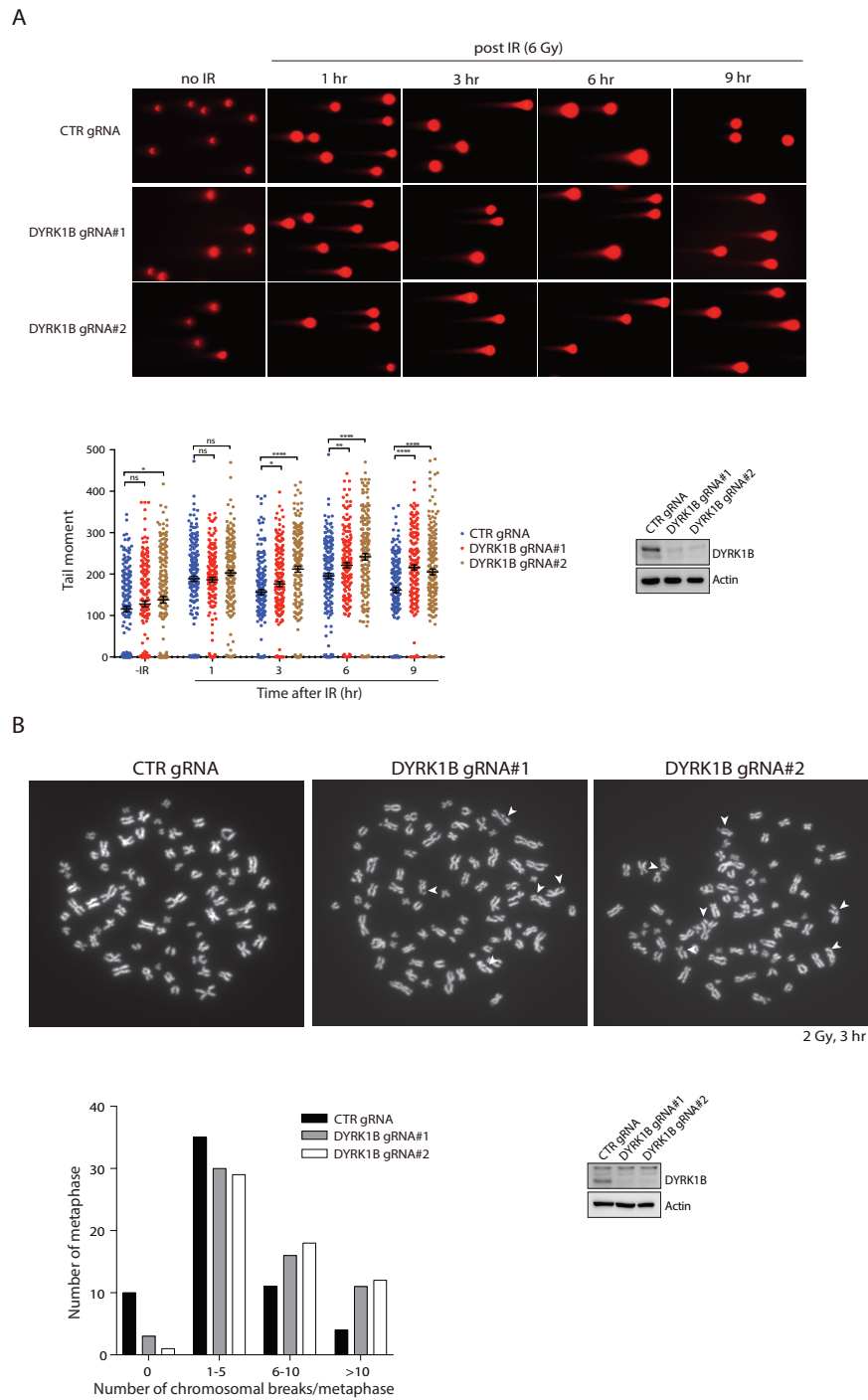
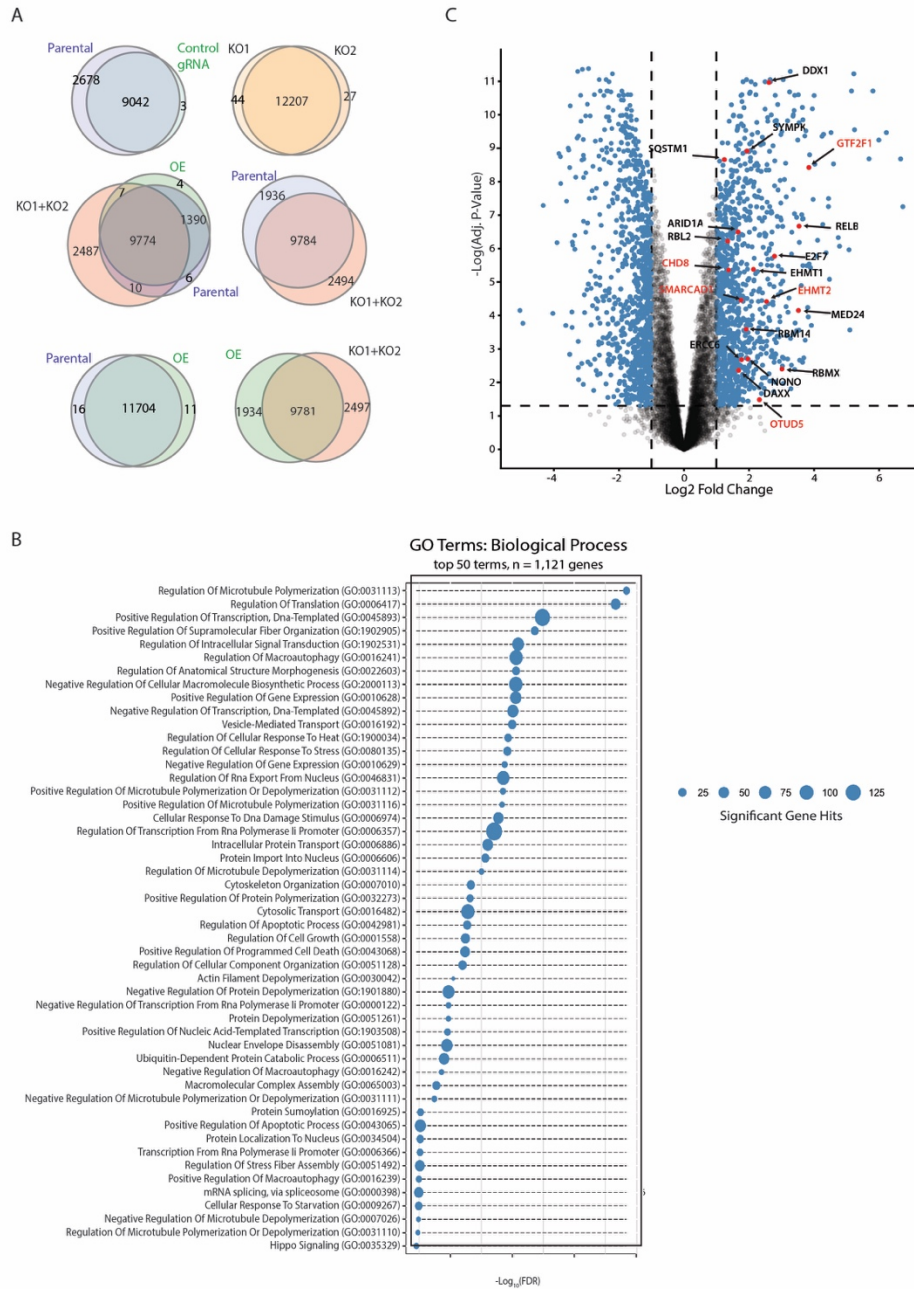




**Figure S5 DYRK1B promotes repair of IR-induced DNA breaks**

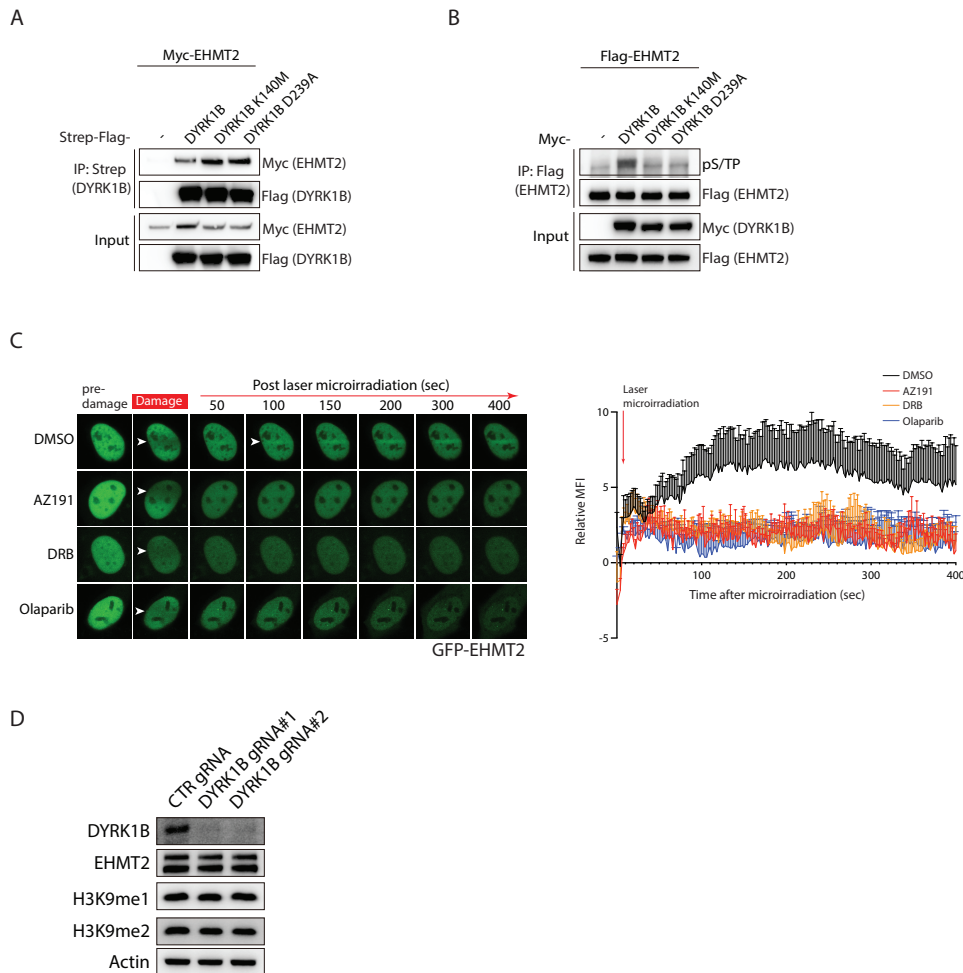
HeLa cells were lenti-virally transduced with control (CTR gRNA) or DYRK1B-targeting gRNAs (DYRK1B gRNA#1 and DYRK1B gRNA#2). Transduced cells were subjected to ionising radiation treatment and were processed for either the Comet assay (**A**) to analyse DNA repair kinetics during cell recovery over a 9-hour period, or for metaphase preparation (**B**) for scoring of chromosomal breaks. For the Comet assay analyses were performed in at least 200 cells from three independent experiments. To score for chromosomal breaks at least 60 metaphases from three independent experiments were counted. Bars represent mean  $\pm$  SEM; \* $P$ <0.05, \*\* $P$ <0.01, \*\*\*\* $P$ <0.0001; ns, not significant. Western blotting experimentations were performed to determine DYRK1B expression in genome-edited cells using indicated antibodies.

Figure S6



**Figure S6 Phospho-profiling of DYRK1B substrates**

**A)** Venn diagrams showing comparison of phosphopeptides identified in each group. Parental vs Control gRNA and KO1 vs KO2 serve as quality control for gRNA effect and experimental variation; **B)** Top 50 biological processes Gene Ontology (GO) terms generated by EnrichR using a list of 1,121 significantly enriched genes from comparison of overexpression (OE) vs knockouts (KO1+KO2). Size of each data point represents total number of identified significant genes within the pathway; **C)** Volcano plot showing the global changes of phosphopeptides in OE vs KO1+KO2 groups. Significantly enriched or depleted phosphopeptides are shown in blue. Phosphopeptides selected for validation are labeled and red text illustrates significant phenotypes. All data represents 4 biological replicates.



**Figure S7 DYRK1B promotes EHMT2 phosphorylation and DSB accumulation**

**A)** DYRK1B interacts with EHMT2. 293T cells transiently transfected with Myc-EHMT2 and Streptavidin binding peptide (Strep)-Flag expression constructs were lysed and processed for co-immunoprecipitation and Western blotting experimentations according to standard procedures; **B)** Cells transiently transfected with indicated expression constructs were lysed and immunoprecipitation using anti-Flag antibodies was performed under denaturing condition. Western blotting was performed using indicated antibodies; **C)** Cells expressing GFP-EHMT2 were pre-treated with indicated inhibitors and time-lapse imaging was performed to analyse EHMT2 accumulation at laser microirradiated sites. Quantification is shown and is derived from at least 10 cells from two independent experiments. Bars represent mean  $\pm$  SEM; **D)** Cells transduced with indicated gRNAs were processed for Western blotting experimentations using indicated antibodies.



**Figure S8 Analysis of metabolic syndrome-derived DYRK1B mutations in DSB repair and in DISC**

**A)** Cells transduced with doxycycline-inducible DYRK1B expression cassettes or vector alone were treated with doxycycline for 24 hours, and were subsequently irradiated (6 Gy) and were allowed to recover for 6 hours before processing for the Comet assay. Tail moment of at least 200 cells from two independent experiments were quantified and results were plotted. Bars represent mean  $\pm$  SEM. \*\*\*\* $P < 0.0001$ . Western blotting was performed to confirm ectopic expression of DYRK1B and its mutants. Asterisk denotes protein band that corresponds to endogenous DYRK1B; **B)** U2OS cells expressing GFP-DYRK1B and mutants were microirradiated and time-lapse imaging was performed to analyse protein accumulation at laser-induced DNA damage tracks. At least 10 cells were analysed from two independent experiments. Bars represent mean  $\pm$  SEM. Western blotting was performed to evaluate steady state expression of DYRK1B alleles; **C)** DYRK1B-inactivated HeLa cells transduced with doxycycline-inducible DYRK1B expression constructs or vector alone were treated with doxycycline for 24 hr, and were subsequently processed for laser microirradiation and immunostaining experimentations using indicated antibodies. Relative 5-EU intensities of 50 cells from three independent experiments are shown. Western blotting was performed to confirm ectopic expression of DYRK1B and its mutants. Asterisk denotes protein band that corresponds to endogenous DYRK1B; **D)** U2OS-DSB reporter cells pre-treated with control (siCTR) or DYRK1B siRNA (siDYRK1B-1) were transiently transfected or not with indicated Myc expression constructs. Cells were subsequently induced with Dox, 4-OHT and Shield-1 and processed for visualisation of mCherry-FokI and YFP-MS2. Quantification of YFP-MS2 mean fluorescence intensity (MFI) is shown and is derived from at least 50 cells from three independent experiments. Bars represent mean  $\pm$  SEM. \*\*\* $P < 0.001$ ; ns, not significant. Western blotting was performed using indicated antibodies.

Figure S9

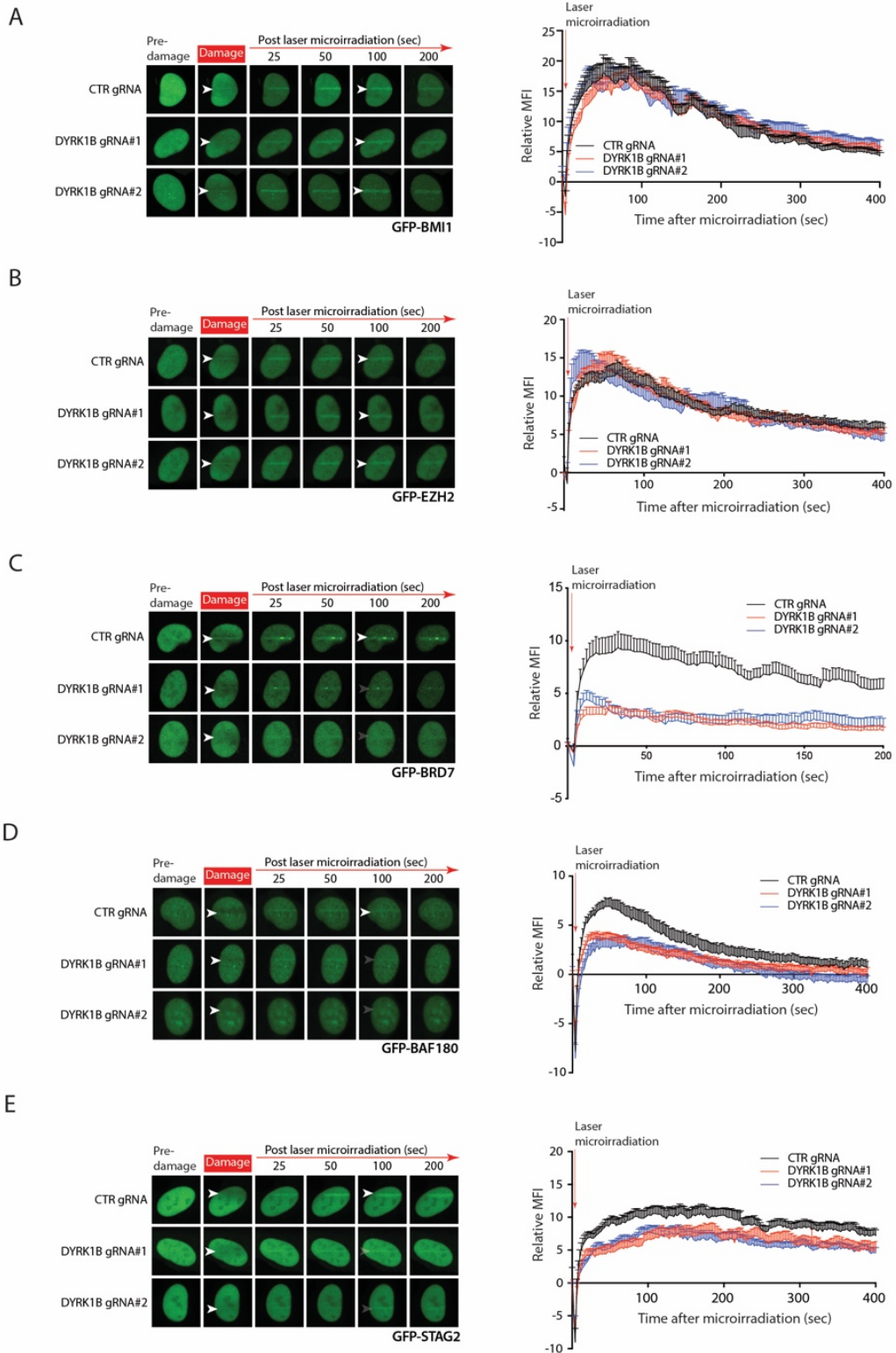


**Figure S9 Analysis of DISC factor accumulation at laser-induced DNA breaks in DYRK1B-inactivated cells**

U2OS cells lenti-virally transduced with control (CTR gRNA) or DYRK1B-targeting gRNAs (DYRK1B gRNA#1 and DYRK1B gRNA#2) were laser microirradiated and time-lapse imaging was performed to analyse accumulation of GFP-tagged BMI1 (**A**), EZH2 (**B**), BRD7 (**C**), BAF180 (**D**) and STAG2 (**E**) at laser microirradiated sites. Quantification is shown and is derived from at least 10 cells from three independent experiments. Bars represent mean  $\pm$  SEM.



Figure S10

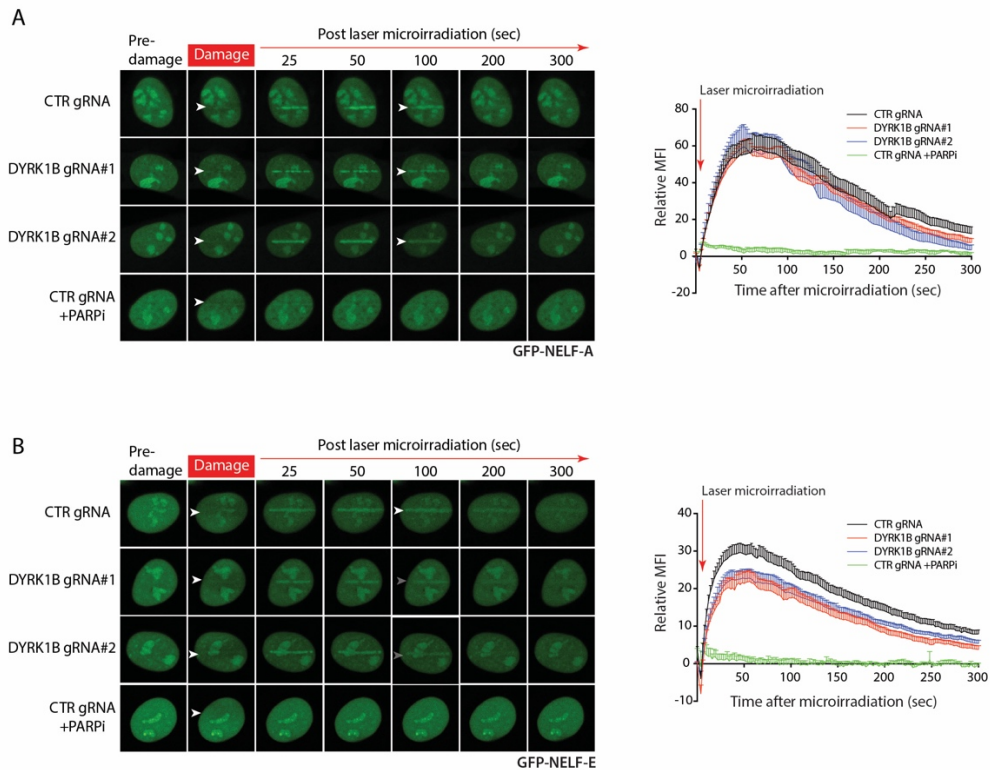


**Figure S10 Analysis of NELF-A/E accumulation at laser-induced DNA breaks in DYRK1B-inactivated cells**

U2OS cells lenti-virally transduced with control (CTR gRNA) or DYRK1B-targeting gRNAs (DYRK1B gRNA#1 and DYRK1B gRNA#2) were laser microirradiated and time-lapse imaging was performed to analyse accumulation of GFP-tagged NELF-A (**A**) and NELF-E (**B**) at laser-induced DSBs. Quantification is shown and is derived from at least 10 cells from three independent experiments. Bars represent mean  $\pm$  SEM. PARP activity was inhibited using Olaparib (PARPi) for 1 hr prior to laser microirradiation.

Figure S11

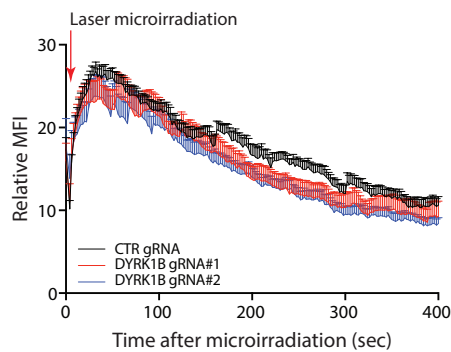
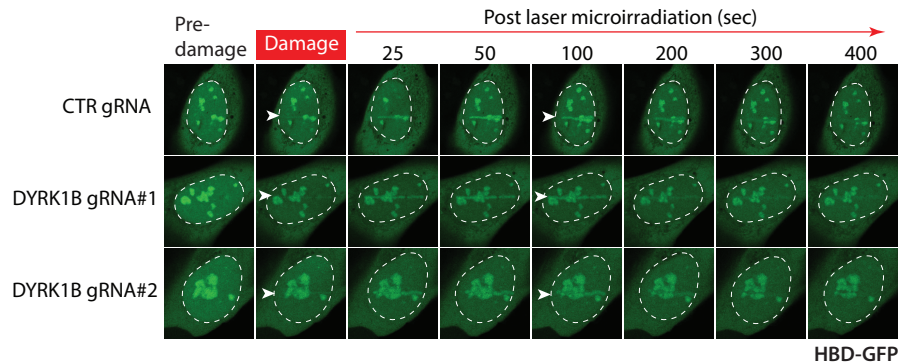


**Figure S11 Analysis of R-loop accumulation at laser-induced DNA breaks in DYRK1B-inactivated cells**

U2OS cells lenti-virally transduced with control (CTR gRNA) or DYRK1B-targeting gRNAs (DYRK1B gRNA#1 and DYRK1B gRNA#2) were transiently transfected with (Hybrid binding domain) HBD-GFP expression construct. HBD is derived from RNaseH1 and was used as a surrogate marker for DNA/RNA hybrids. Quantification is shown and is derived from at least 10 cells from two independent experiments. Bars represent mean  $\pm$  SEM.

**Table S1 List of chemicals used in this study**

<b>Chemical</b>	<b>Source</b>	<b>Identifier</b>
AZ191	Selleckchem	S7338
KU-55933	Selleckchem	S1092
VE-821	Selleckchem	S8007
CX5461	Selleckchem	S2684
UNC0638	Selleckchem	S8071
5,6-Dichloro-1- $\beta$ -D-ribofuranosylbenzimidazole, DRB	Sigma-Aldrich	D1916
$\alpha$ -amanitin	Sigma-Aldrich	A2263
Actinomycin D	Sigma-Aldrich	A1410
DMSO	Sigma-Aldrich	D2650
Doxycycline hyclate	Sigma-Aldrich	D9891
Olaparib	Selleckchem	S1060
4',6-diamidino-2-phenylindole, DAPI	Thermo Fisher Scientific	D1306
Hexadimethrine bromide	Sigma-Aldrich	107689
Geneticin (G418) sulfate	ChemCruz	Sc-29065B
Shield1	TaKaRa	632189
(Z)-4-Hydroxytamoxifen	Sigma-Aldrich	H7904
Colcemid solution	Thermo Fisher Scientific	15210040
Benzonase Nuclease	ChemCruz	sc-202391
Puromycin dihydrochloride	Sigma-Aldrich	P8833
Coomassie Brilliant Blue R-250	Affymetrix, Thermo Fisher Scientific	6104-59-2
Oligofectamine	Invitrogen	12252-011
Anti-Flag Affinity Gel	Bimake.com	B23102
Streptavidin Sepharose High Performance affinity resin	GE Healthcare	17-5113-01
Propidium iodide	Sigma-Aldrich	P4170
Polyethylenimine	Polysciences	23966

**Tables S2 List of plasmids used in this study**

<b>Plasmid</b>	<b>Source</b>	<b>Identifier</b>
pDONR223-DYRK1B	Addgene	Plasmid #23761
Non-targeting control gRNA	Addgene	Plasmid #80248
DYRK1B gRNA#1	Addgene	Plasmid #76621
DYRK1B gRNA#2	Addgene	Plasmid #76623
LentiCas9-Blast	Addgene	Plasmid #52962
LentiCRISPR v2	Addgene	Plasmid #52961
GFP-BRD7	Addgene	Plasmid #65379
GFP-BAF180	Addgene	Plasmid #65387
pFRT- TODestGFP_RNAseH1	Addgene	Plasmid #65784
EHMT2 cDNA	Harvard PlasmID Database	HsCD00329370
EZH2 cDNA	Harvard PlasmID Database	HsCD00039865
BMI1 cDNA	Harvard PlasmID Database	HsCD00000297
GFP-NELF-A	Gift from Nabieh Ayoub	N/A
GFP-NELF-E	Gift from Nabieh Ayoub	N/A
pEGFP-STAG2	Gift from Jessica A. Downs	N/A
pEGFP-C1-53BP1	Gift from Simon Bekker- Jensen	N/A
psPAX2	Addgene	Plasmid #12260
pMD2.G	Addgene	Plasmid #12259
pMH-SFB	Addgene	Plasmid #99391
pMH-MYC	Addgene	Plasmid #101765
pMH-SFB-DYRK1B	Addgene	Plasmid #101771
pMH-CMV-GFP	Addgene	Plasmid #133017

**Table S3 Details of antibodies used in this study**

<b>Antibody</b>	<b>Source</b>	<b>Identifier</b>
Mouse monoclonal anti-RNA polymerase II 8WG16	Covance	MMS-126R
Rabbit polyclonal to RNA polymerase II CTD repeat YSPTSPS (phospho S2)	Abcam	ab5095
Rabbit polyclonal to RNA polymerase II CTD repeat YSPTSPS (phospho S5)	Abcam	ab5131
Rat monoclonal RNA pol II CTD phosphor Ser7 antibody (4E12)	Active Motif	61087
Mouse monoclonal anti- $\beta$ -Actin	Sigma-Aldrich	A5441
Rabbit monoclonal anti-DYRK1B(D40D1)	Cell Signaling Technology	5672
Mouse monoclonal anti-DYRK1B(H-6)	Santa Cruz	sc-390417
Mouse monoclonal anti- $\gamma$ H2AX	In-house	N/A
Rabbit monoclonal anti- $\gamma$ H2AX	In-house	N/A
Mouse monoclonal anti-Flag (M2)	Sigma-Aldrich	F3165
Anti-Ubiquitinated proteins, clone FK2	EMD Millipore	04-263
Anti-Ubiquitin, Lys63-specific, clone Apu3	EMD Millipore	05-1308
Peroxidase AffiniPure Rabbit Anti-mouse IgG+IgM (H+L)	Jackson ImmunoResearch	315-035-048
Peroxidase AffiniPure Goat Anti-Rabbit IgG (H+L)	Jackson ImmunoResearch	111-035-144
Goat anti-Mouse IgG (H+L) Cross-Adsorbed Secondary Antibody, Alexa Fluor 405	Thermo Fisher Scientific	A-31553
Goat anti-Rabbit IgG (H+L) Cross-Adsorbed Secondary Antibody, Alexa Fluor 405	Thermo Fisher Scientific	A-31556
Alexa Fluor 594 AffiniPure Goat Anti-Mouse IgG (H+L)	Jackson ImmunoResearch	115-585-166
Alexa Fluor 488 AffiniPure Goat Anti-Rabbit IgG (H+L)	Jackson ImmunoResearch	111-545-144
Anti-phospho-Ser/Thr-Pro, MPM-2	EMD Millipore	05-368
Anti-Histone H3 (mono methyl K9) antibody	Abcam	ab9045
Anti-Histone H3 (di methyl K9) antibody	Abcam	ab1220
EHMT2 (C6H3) Rabbit mAb	Cell Signaling Technology	3306
Anti-ubiquityl-Histone H2A Antibody, clone E6C5	EMD Millipore	05-678
c-Myc Antibody (9E10): sc-40	Santa Cruz	sc-40
GFP Antibody	Cell Signaling Technology	2555

**Table S4 Sequences of siRNAs used in this study**

<b>siRNA</b>	<b>Sequence</b>
siControl	UAGCGACUAAACACAUCA
siDYRK1B#1	GUGGUGAAAGCCUAUGAUCAUUU
siDYRK1B#2	CGAAAGAACUCAGGAAGGAUU
siOTUD5#1	GGACGAACCCAUUCGUGUUTT
siOTUD5#2	GGAGGAGUCAUGGAUUGAATT
siOTUD5#3	GCUCUUGCCAAACCUCCUUTT
siARID1A#1	GCCCUAACAUUGGCCAAUAUTT
siARID1A#2	GCAGGCACCACUAACUUAUTT
siARID1A#3	GCAGGAGCUAUCUCAAGAUTT
siEHMT1#1	CGGUGAUUGAGAUGUUUAATT
siEHMT1#2	GGUUCUGAGUCGUUAAGUTT
siEHMT1#3	CAGCAACGGAUACAUCUUATT
siEHMT2#1	GGUUUGCGCUUCAACUCAATT
siEHMT2#2	GCAUAGAUGCCCGUUACUATT
siEHMT2#3	GGUCUUCAUGCUGCACCATT
siGTF2F1#1	GCAAGAUGAUCAACGACAATT
siGTF2F1#2	GGAGGAACAAGGUGCUGAATT
siGTF2F1#3	GCAGCCGACAAAGUCAACUTT
siRELB#1	GCCCGUCUAUGACAAGAAATT
siRELB#2	GGAAGAUUCAACUGGGCAUTT
siRELB#3	GCUGCGGAUUUGCCGAAUUTT
siMED24#1	GCUGCACAUCGCCAAACUATT
siMED24#2	GCGAAGACAUUGAGGAUUATT
siMED24#3	GCAGCGAAGAAAGCACCAATT
siRBMX#1	GCCAGAGACAUGAAUGGAATT
siRBMX#2	GCUAUUCAAGCAGAGAUUATT
siRBMX#3	GGUCGUGAUCGUGACUAUUTT
siRBM14#1	GCUCCUAUAUGAUUACCUUTT
siRBM14#2	GCAAAGAAGUGAAGGGCAATT
siRBM14#3	GGCCUCUUAUACUUGGAATT
siE2F7#1	GCUGCCAGCCCAGAUUAUATT
siE2F7#2	GCAGUCUCCUGCAGGAUUATT
siE2F7#3	GCAUCUGUCUUACCAGAAUTT
siRBL2#1	GCCCUGUACUGUGUCUGAATT
siRBL2#2	GCGGAGAUGCUIUACUAUATT
siRBL2#3	GCGGCUAUUUGUUGAGAAUTT
siERCC6#1	GCACGUUGCCUGUGUUUAUTT
siERCC6#2	CCUAAGAACUCUAAGCAUUTT
siERCC6#3	GCAUGUGUCUACGAGAUATT
siDDX1#1	GGAGUUAGCUGAACAAACUTT
siDDX1#2	GAGCCACAUUAGAACUGAUTT
siDDX1#3	GCUGAACUGAAAUUUAACUTT

siNONO#1	GAGGUGCUAUGGGCAUAAATT
siNONO#2	GGCGAAGUCUUCAUUCAUATT
siNONO#3	GGAAGGCACUCAUUGAGAUTT
siSMARCAD1#1	GACGGCUGAAACUUAUUATT
siSMARCAD1#2	GAUGGAGGAUGGCUAUAATT
siSMARCAD1#3	GGCUGGCAUUGGUACAUAATT
siCHD8#1	GGAUCAGAUGAACCAGGAUTT
siCHD8#2	CCAAGUACUUCCAUGGCUUTT
siCHD8#3	GCAGUUACACUGACCUCUATT
siDAXX#1	GCUCUAUGUCUACAUAUATT
siDAXX#2	CCACCUCACAGAUGACUAUTT
siDAXX#3	GCAUUGAGCGGCUCAUCAATT
siSQSTM1#1	GGAACAGAUGGAGUCGGAUTT
siSQSTM1#2	CCUACGUGAAGGAUGACAUTT
siSQSTM1#3	CCAGACUACGACUUGUGUATT
siSYMPK#1	GCUCUUGAGGGACGAGAAUTT
siSYMPK#2	GCGGGAGUAUGUGGAGAAATT
siSYMPK#3	GCCAGAGACCCAUGUUCAUTT
siELL#1	GCCAGACAGGAUUCUGUUUTT
siELL#2	GCCGAAGUGCCAUUGUCAUTT
siELL#3	GCACUUCACUCAGAGAGCUTT
siYAF2#1	CCACCCGAUCCACAUUGUUTT
siYAF2#2	CCAAGGAACCGUUGAAAUUTT
siYAF2#3	GCAGUUUGGCCUCCUACATT
siSMARCA2#1	GCUCUUUGCCACCAGAUUUTT
siSMARCA2#2	GCAGCAGACCGAUGAGUAUTT
siSMARCA2#3	GCGUCUACAUAAGGUGUUATT
siPAF1#1	GCCGAGUCAAGUACUGCAATT
siPAF1#2	CCGUUAUGGCAUCUCCAAUTT
siPAF1#3	GGAGAUCUUUGGCAGUGAUTT

---

**Table S5 Sequences of gRNAs used in this study**

<b>CRISPR gRNA</b>	<b>Sequence</b>
Non-targeting control gRNA	GTATTACTGATATTGGTGGG
DYRK1B#1	CATGACTACATCGTGCGCAG
DYRK1B#2	AGGCTCGCAAGTACTTTGAA
EHMT2#3	GGGTCACTTCTCCTGAACGC
EHMT2#4	CACGCGCTCATCCACAGAGT